Icarus 243 (2014) 296–310

Contents lists available at ScienceDirect

Icarus

journal homepage: www.elsevier.com/locate/icarus

Origin and development of theater-headed valleys in the Atacama Desert, northern Chile: Morphological analogs to martian valley networks

Rossman P. Irwin III [a,*], Stephen Tooth [b], Robert A. Craddock [a], Alan D. Howard [c], Ana Baptista de Latour [d]

[a] Center for Earth and Planetary Studies, National Air and Space Museum, Smithsonian Institution, MRC 315, 6th St. at Independence Ave. SW, Washington, DC 20013, USA
[b] Department of Geography and Earth Sciences, Aberystwyth University, Ceredigion, SY23 3DB Wales, UK
[c] Department of Environmental Sciences, P.O. Box 400123, University of Virginia, Charlottesville, VA 22904-4123, USA
[d] Consultante Grands Comptes, ESRI France, 21, Rue des Capucins, 92195 Meudon Cedex, France

ARTICLE INFO

Article history:
Received 25 October 2013
Revised 7 August 2014
Accepted 11 August 2014
Available online 21 August 2014

Keywords:
Mars, surface
Earth
Geological processes

ABSTRACT

Understanding planetary landforms, including the theater-headed valleys (box canyons) of Mars, usually depends on interpreting geological processes from remote-sensing data without ground-based corroboration. Here we investigate the origin and development of two Mars-analog theater-headed valleys in the hyperarid Atacama Desert of northern Chile. Previous workers attributed these valleys to groundwater sapping based on remote imaging, topography, and publications on the local geology. We evaluate groundwater sapping and alternative hypotheses using field observations of characteristic features, strength measurements of strata exposed in headscarps, and estimates of ephemeral flood discharges within the valleys. The headscarps lack evidence of recent or active seepage weathering, such as spring discharge, salt weathering, alcoves, or vegetation. Their welded tuff caprocks have compressive strengths multiple times those of the underlying epiclastic strata. Flood discharge estimates of cubic meters to tens of cubic meters per second, derived using the Manning equation, are consistent with the size of transported clasts and show that the ephemeral streams are geomorphically effective, even in the modern hyperarid climate. We interpret that headscarp retreat in the Quebrada de Quisma is due to ephemeral flood erosion of weak Miocene epiclastic strata beneath a strong welded tuff, with erosion of the tuff facilitated by vertical jointing. The Quebrada de Humayani headscarp is interpreted as the scar of a giant landslide, maintained against substantial later degradation by similar strong-over-weak stratigraphy. This work suggests that theater-headed valleys on Earth and Mars should not be attributed by default to groundwater sapping, as other processes with lithologic and structural influences can form theater headscarps.

Published by Elsevier Inc.

1. Introduction

The martian landscape has compelling analogs in both hot and cold deserts on Earth, particularly in very arid regions with little recent erosion by surface water (e.g., Chapman, 2007). The preservation of ancient cratered terrain in the southern highlands shows that Mars has been hyperarid for about 75% of its history, although it experienced wetter conditions at least intermittently prior to about 3.0–3.6 Ga (e.g., Malin, 1976; Carr and Clow, 1981; Golombek et al., 2006; Fassett and Head, 2008; Grant and Wilson, 2011). The highlands contain fluvially degraded impact craters and branching valley networks, most of which drained to enclosed basins (e.g., Maxwell and Craddock, 1995; Craddock et al., 1997). Most fluvial valleys are incised ~50–350 m into sparsely dissected intercrater geomorphic surfaces that formed during the Middle to Late Noachian Epochs (Howard et al., 2005). On these intercrater surfaces, martian fluvial valleys commonly have a theater-shaped headscarp and steep sidewalls with relatively little dissection by gullies (e.g., Pieri, 1980). Valley cross sections are locally V-shaped (particularly on steeper regional slopes, e.g., Fig. 1) but more commonly are trapezoidal, with a flat floor (Baker and Partridge, 1986; Goldspiel et al., 1993; Williams and Phillips, 2001).

By analogy with some morphologically similar theater-headed valleys (box canyons) on Earth, many workers have attributed these characteristics to groundwater sapping, a term that encapsulates seepage-related weathering processes and erosion of the resulting debris by spring discharge (e.g., Pieri, 1980; Mars

* Corresponding author.
E-mail addresses: irwinr@si.edu (R.P. Irwin III), set@aber.ac.uk (S. Tooth), craddockb@si.edu (R.A. Craddock), ah6p@virginia.edu (A.D. Howard).

http://dx.doi.org/10.1016/j.icarus.2014.08.012
0019-1035/Published by Elsevier Inc.

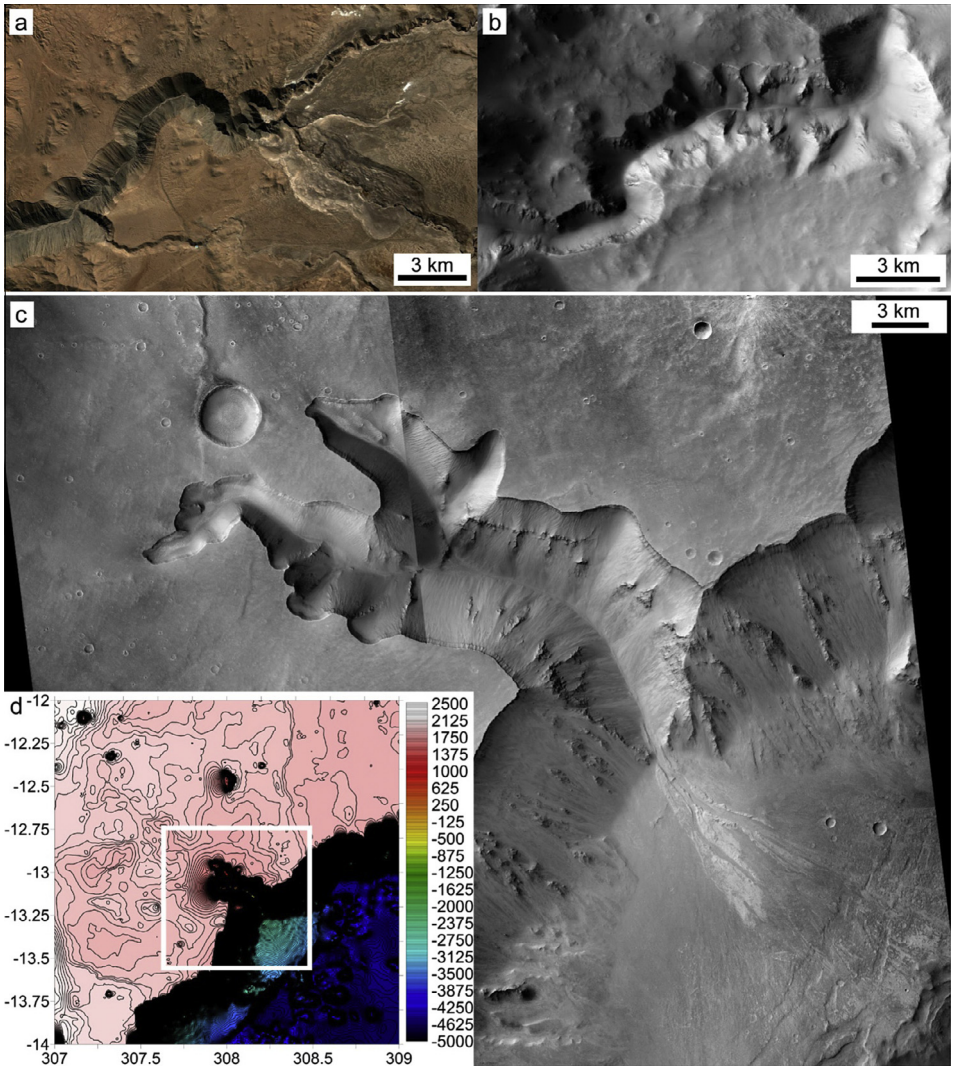

Fig. 1. Comparison of (a) Quebrada de Tiliviche (19.5°S, 70.5°W, Google Earth, flow toward the left) with (b) a martian fluvial valley (5.4°S, 134.7°E, Mars Reconnaissance Orbiter Context Camera, flow toward the right). In both cases, note the deeply incised valley and poorly dissected interfluve areas. (c) Theater-headed valleys in the Valles Marineris region of Mars, 13.2°S, 51.9°W, provided for comparison with the smaller Quebrada de Quisma in Fig. 5a. Mars Reconnaissance Orbiter Context Camera images P08_004027_1645 and P15_006796_1649. (d) Mars Orbiter Laser Altimeter topography (25 m contour interval) of the area shown in Fig. 1c (white outline) and surroundings. Note the plateau slope toward the valley heads. North is up in this and all subsequent plan view figures.

Channel Working Group, 1983; Brakenridge, 1990; Malin and Carr, 1999; Harrison and Grimm, 2005). Laity and Malin (1985, p. 203) defined groundwater sapping as "the process leading to the undermining and collapse of valley head and side walls by weakening or removal of basal support as a result of enhanced weathering and erosion by concentrated fluid flow at a site of seepage." On Earth, seepage weathering can enable retreat of a vertical headscarp by undermining of the base, through processes including physical weathering (e.g., salt weathering or freeze thaw), chemical weathering, or root growth at a seepage face. Spring discharge and/or surface runoff are invoked as the processes that remove the weathered debris and any mass-wasted materials (Dunne, 1980; Laity, 1983; Higgins, 1984; Laity and Malin, 1985; Howard et al., 1988). If valley weathering and erosion by spring discharge alone were possible under a cold, arid climate, then the groundwater sapping interpretation could have significant implications for the paleoclimate of early Mars (e.g., Gaidos and Marion, 2003).

Interpretations of groundwater sapping on Mars have been controversial, however, as dissection on Mars is locally dense (e.g., Hynek and Phillips, 2003; Mangold et al., 2004) and many tributary heads occur near drainage divides (e.g., Masursky et al., 1977; Craddock and Howard, 2002; Carr, 2002). For both of these reasons, available contributing aquifers would have been small. In addition, significant aquifer recharge would have been needed to transport the weathered volume of debris equivalent to martian valley volumes (Howard, 1988; Gulick and Baker, 1990; Goldspiel and Squyres, 1991; Goldspiel et al., 1993; Grant, 2000; Gulick, 2001; Craddock and Howard, 2002). Alternative explanations for steep or vertical valley headscarps in terrestrial bedrock have been noted, including surface flood erosion of strong-over-weak stratigraphy or vertically jointed rock, although very large floods ('megafloods') may be required to topple columns of jointed rock (Lamb et al., 2008a, 2014; Lamb and Dietrich, 2009). Flood erosion of strong-over-weak stratigraphy can involve undercutting of the headscarp caprock at or around waterfall plunge pools (e.g., Lamb et al., 2006, 2007). The latter studies suggest that a groundwater sapping origin of bedrock valleys may not have been uniquely demonstrated anywhere on Earth, and that a positive relationship between spring discharge and weathering rate similarly lacks empirical support. However, groundwater sapping in unconsolidated materials has been demonstrated in the laboratory (Howard and McLane, 1988; Marra et al., 2014) and in at least one

field setting in Florida, where it is less controversial than sapping in bedrock (Schumm et al., 1995; Lobkovsky et al., 2007; Perron and Hamon, 2012). These explanations are not mutually exclusive, and more than one may apply in a given location. Moreover, as we discuss below, the physical processes that initially form a headscarp may be different from those that subsequently maintain or develop the landform.

The use of Earth analogs to improve process understanding of morphologically similar features on Mars depends on a correct analysis of the origin and development of the Earth analogs. The purpose of this study is to evaluate whether a groundwater sapping origin for development of theater-headed valleys on Earth can be confidently inferred using only data sources that are similar to those currently available for Mars: plan-view images, remotely sensed topography, and geologic context. The study sites are in the Atacama Desert of northern Chile (Fig. 2), which has arguably experienced more prolonged and severe aridity than any other region on Earth (Hartley et al., 2005; Dunai et al., 2005; Clarke, 2006). Hoke et al. (2004) inferred a groundwater sapping origin for three theater-headed quebradas (i.e., valleys or canyons, although the Spanish word does not necessarily imply a theater headscarp) that cross the desert from the Andes westward to the Pacific Ocean (18–19.5°S) or to enclosed basins (>19.5°S) (Fig. 2). They noted that the "dominant diagnostic features seen in images and topographic data are (1) deeply incised canyon networks (that crosscut an older parallel drainage network)..., (2) upstream terminations of the canyons at pronounced headwalls or relict headwalls..., and (3) springs at the base of the western slope.... The nonbifurcating nature of the network is a typical feature of sapping valleys observed in both laboratory and field studies...." (Hoke et al., 2004, p. 607). Their data included: images from the Landsat Thematic Mapper and the Advanced Spaceborne Thermal Emission Radiometer (ASTER); 20-m/pixel topography derived from the European Remote-Sensing Satellite (ERS) 1 and 2 radar; and publications on the stratigraphy, hydrology, and geomorphology of the area. They did not, however, report field observations. Consequently, these valleys offer a valuable field test of interpretations that were based largely on remote-sensing data, with implications for the interpretation of similar landforms elsewhere on Earth and on Mars.

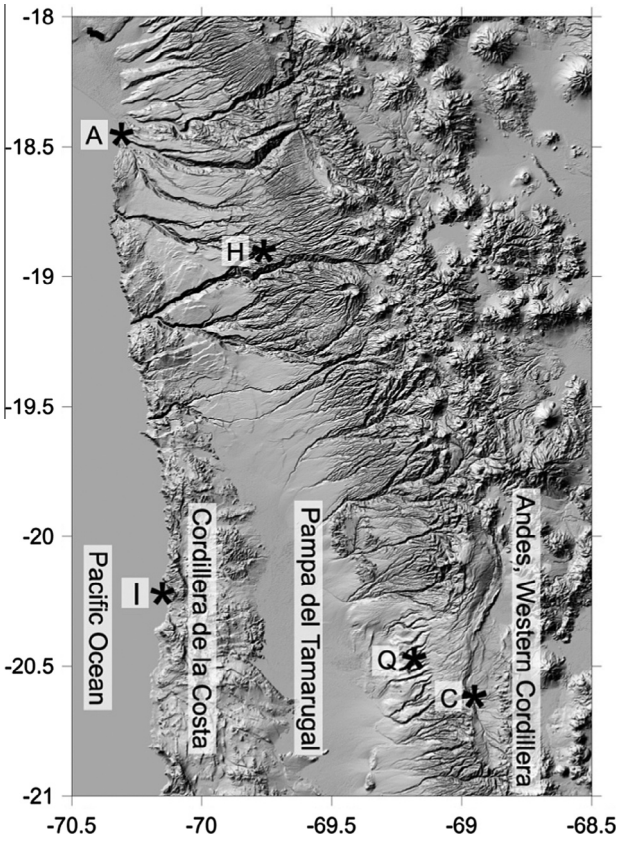

Fig. 2. Shuttle Radar Topography Mission shaded relief map (93 m/pixel, unprojected) with major physiographic features labeled. Also shown are the locations of two major Chilean cities, Arica (A) and Iquique (I), and the three quebradas studied by Hoke et al. (2004) and discussed in the text: Humayani (H), Quisma (Q), and Chacarilla (C).

2. Study area

2.1. Regional setting

The Atacama Desert is extremely dry due to a combination of topography, atmospheric circulation, and ocean currents (e.g., Houston and Hartley, 2003). The descending Hadley circulation and easterly winds at this latitude (~20°S) combine with continentality and the Andean rain shadow to inhibit precipitation. The cold Humboldt Current runs northward along the Pacific coast, cooling the near-surface air and creating a stable temperature profile, so moist air is trapped along the coast. In northern Chile, the annual precipitation and resulting fluvial dissection decline rapidly westward, with annual rainfall ranging from ~20 cm/a at higher elevations to <0.1 cm/a near the coast (Houston and Hartley, 2003; Houston, 2006; Strecker et al., 2007; García et al., 2011). Long-term semiarid to hyperarid climates, arguably since the late Triassic (Clarke, 2006) or late Jurassic (Hartley et al., 2005), has combined with rapid uplift of the Andes since the Miocene (when the rain shadow and aridity were enhanced) to create a landscape in which tectonic features are unusually well expressed on the surface (Gregory-Wodzicki, 2000; Rech et al., 2006).

Under these conditions, the large quebradas of northern Chile developed with similar morphology to martian valley networks (e.g., Mortimer, 1980) (Figs. 1 and 2). The quebradas have V-shaped to trapezoidal cross sections, and they typically possess few tributaries except in steep headwater areas. The quebradas have low sinuosity, display only limited sidewall dissection, undergo little downstream widening in most cases, and are flanked by poorly dissected to undissected interfluve surfaces along their lower reaches (Figs. 1a and 2). Intermittent runoff from the Andean headwaters is the only significant water source for most of the quebradas (e.g., Houston, 2006), so the few locally sourced tributaries to the lower reaches are typically shallow, very infrequently active, hanging, and partly mantled by aeolian sand.

The exorheic quebradas (i.e., draining to the ocean rather than to enclosed continental basins) from 18 to 19.5°S crosscut a parallel drainage network that formed between 15.0 ± 0.6 and 11.2 ± 0.6 Ma, whereas those endorheic quebradas (i.e., draining to enclosed basins) south of 19.5°S have incised alluvial sediments that were deposited about 6 Ma (García et al., 2011). García et al. (2011) attributed these age relationships to less runoff in the southern headwater areas than in the north, thus arguing for the later establishment of exorheic drainage. They concluded that the quebrada incision was more due to periods of semiarid (i.e., wetter) paleoclimate in the headwaters than to uplift during the time of incision.

For these reasons, geomorphic surfaces in the Atacama Desert have variable ages that depend on their last exposure to runoff from the east (e.g., Alpers and Brimhall, 1988; Hartley and Chong, 2002; Dunai et al., 2005; Evenstar et al., 2009). The Cordillera de la Costa (Fig. 2) is a low range (generally <2000 m) with an abrupt scarp facing the Pacific Ocean. This range includes the

region's oldest geomorphic surfaces, which are up to ~25 Ma in age (Dunai et al., 2005). In this area, old gullies and steep slopes are devoid of vegetation but mantled by sand and silt, owing to a lack of sufficient runoff to remove weathered debris and wind-blown material. Inland is a north–south band of enclosed basins and alluvial deposits called the Pampa del Tamarugal, which receives some ephemeral floods from the Andes to the east but very little direct precipitation. Locally, groundwater tables in these basins are shallow and support isolated groves of phreatophyte trees (e.g., Mooney et al., 1980). Farther inland, a long incline mantled by dissected alluvial deposits with a range of ages (22–1.2 Ma, with fluvial activity slowing after 14.6 Ma) rises toward the Western Cordillera of the Andes (Evenstar et al., 2009). This feature is commonly termed the Atacama Planation Surface. Although the Atacama Desert has preserved Miocene and younger geomorphic surfaces, fluvial dissection in the Andes and sedimentary deposition in parts of the Pampa del Tamarugal are ongoing, and the landscape cannot be considered relict in its entirety.

2.2. Study sites

On the Atacama Planation Surface, Hoke et al. (2004) illustrated three specific valleys with a morphology that they attributed to groundwater sapping. From north to south, these valleys are the Quebrada de Humayani, the Quebrada de Quisma, and the Quebrada de Chacarilla (Fig. 3). The former is a tributary to the Quebrada de Camarones, which drains to the Pacific Ocean, whereas the latter two debouch to the enclosed Pampa del Tamarugal. We focused field data collection and analysis on the Quebrada de Humayani and the Quebrada de Quisma, but in the discussion, we also include remote-sensing observations and data from previously published studies of the Quebrada de Chacarilla for comparative purposes. Other theater-headed valleys are also found in the region (e.g., around 19.27°S, 69.63°W, about 40 km south of the Quebrada de Humayani), but they were not a focus of either this study or that of Hoke et al. (2004).

The Quebrada de Humayani headwaters arise in the breached crater and on the northwest flank of a partially eroded Miocene volcano at ~3500–4200 m elevation (crater centered at 18.85°S, 69.38°W, Fig. 3a). About 45 km downstream, the quebrada contains a transverse scarp 3 km wide and 200 m high, with a top at 1850–1950 m elevation (18.910°S, 69.764°W, Fig. 4). Members 1 and 2b of the upper Oligocene–lower Miocene Oxaya Formation are exposed in this scarp (members of this and other formations described here increase in number up-section) (García et al., 2004). Member 1 includes ignimbrites with variable degrees of welding and other interbedded sedimentary rocks (mostly sandstones and conglomerates, but some limestones and dolomites). Using Ar–Ar in sanidine, the upper Oligocene basal tuff of Member 1 was dated to 24.7 ± 0.3 Ma (García et al., 2004). The overlying Miocene Member 2b is the Oxaya Ignimbrite, which García et al. (2004) described as a regionally extensive, rhyolitic, pyroclastic flow unit that varies between 20 and 200 m thick and thins toward the west. The member includes: (1) three lower layers of gray and pink, massive, unwelded pyroclastic flow deposits totaling a few tens of meters thick; (2) a pinkish brown, moderately to highly

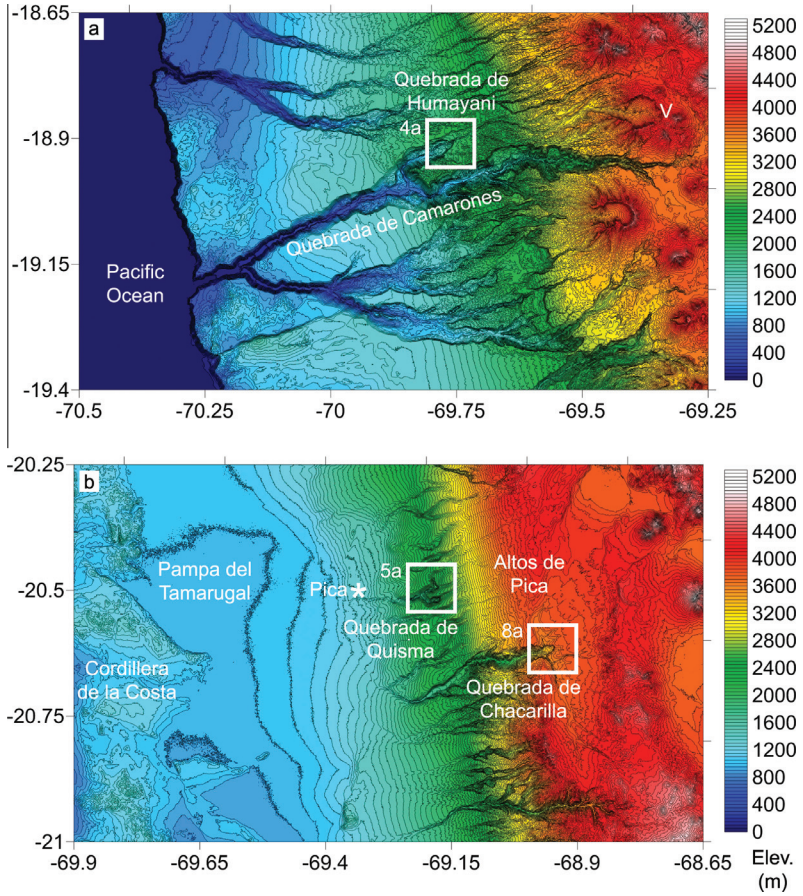

Fig. 3. Shuttle Radar Topography Mission contour maps (93 m/pixel, 50 m interval, unprojected) of study areas and their surroundings. (a) Vicinity of Quebrada de Humayani, indicating area of Fig. 4a. The Quebrada de Humayani is sourced in and around a volcano (V) and drains to the Pacific Ocean via Quebrada de Camarones. (b) Vicinity of Quebradas de Quisma and Chacarilla, indicating areas covered by Figs. 5a and 8a. These quebradas drain to the inland basin of the Pampa del Tamarugal, which is bounded to the west by the Cordillera de la Costa.

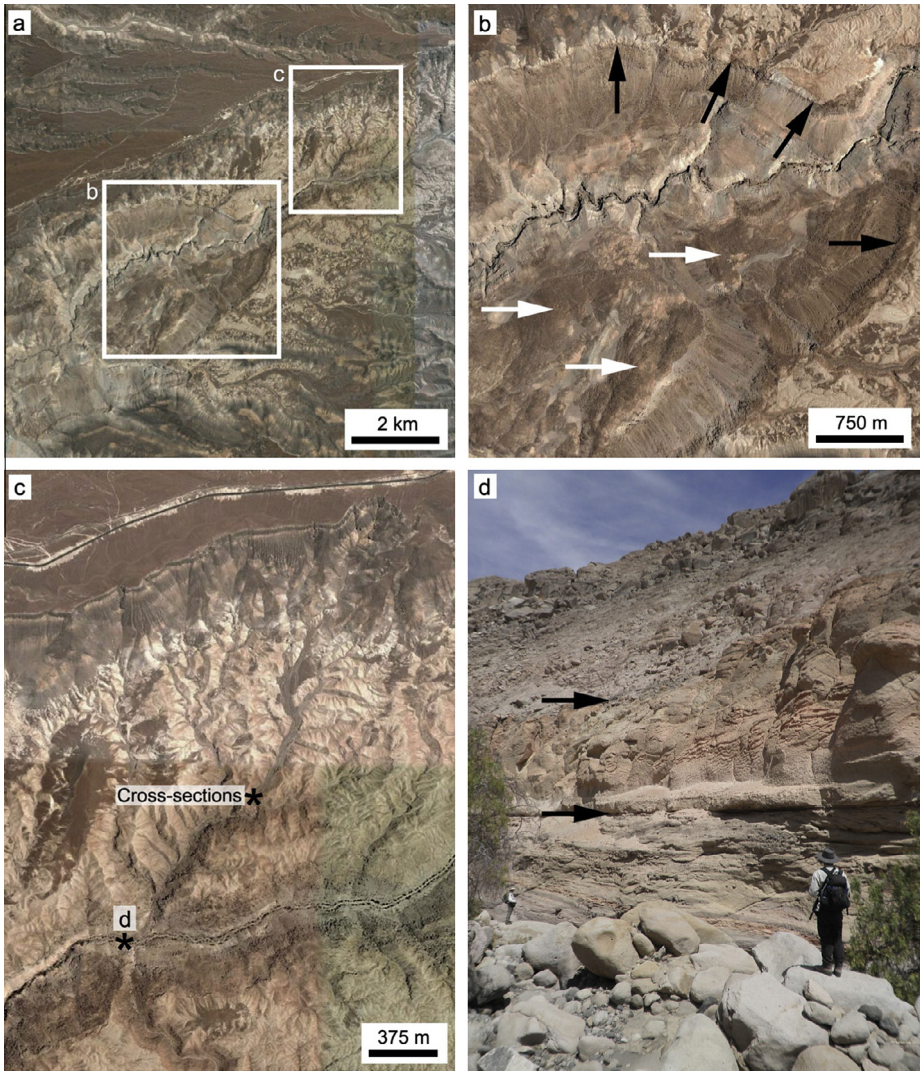

Fig. 4. Quebrada de Humayani. (a) Overview of headscarp area (Google Earth imagery), indicating areas covered by (b and c). (b) Enlargement of headscarp (Google Earth imagery), with black arrows indicating outcrop of welded tuff and white arrows indicating major slump blocks of the mass wasting deposits. (c) Tributary where discharge estimates were made, showing location of two channel cross sections (both at this point, a short distance apart) and location of (d). (d) Epiclastic strata (bottom), pink ignimbrite (center) and resistant gray welded tuff (top) submembers of the Oxaya Ignimbrite exposed in north canyon wall, with the two major contacts indicated by arrows. Note the bouldery bed of the master stream, which indicates substantial discharge during flash floods. (For interpretation of the references to color in this figure legend, the reader is referred to the web version of this article.)

welded, massive, homogeneous pyroclastic flow, 150 m thick; and (3) a light gray, unwelded, pumice-rich upper layer, <20 m thick. Based on three Ar–Ar ages in sanidine, the member formed about 19.4 Ma (García et al., 2004). The physical properties of ignimbrites described in the northern Atacama Desert typically vary within and between mapped members (e.g., Dingman and Galli, 1965), and where we refer to a welded tuff, it is typically a member or submember of a thicker ignimbrite deposit.

The Quebrada de Quisma (20.473°S, 69.185°W, Fig. 5) heads on the Altos de Pica plateau above 4000 m elevation, and it drains to the Pampa del Tamarugal near Pica (Fig. 3b). The Altos de Pica Formation is primarily a continental sedimentary sequence derived from late Tertiary erosion of the Andes. Ignimbrites thicken toward higher elevations, whereas alluvial (plus some aeolian) strata thicken downslope, and these pyroclastic and epiclastic strata interfinger at mid-slope. The Altos de Pica Plateau receives over 20 cm of precipitation per year, and the formation's permeability makes it the essential aquifer for the town of Pica. At 1300 m elevation, Pica receives on average only 1–2 cm of light rain per year, but it contains several springs that collectively discharge about 53 L/s. Elsewhere in the area, springs from the Altos de Pica Formation are found only at Chacarilla (Galli and Dingman, 1962; Dingman and Galli, 1965).

The Quebrada de Quisma headscarp is about 23 km downstream of the headwaters and is 100 m wide and 60 m high, with an upper surface at 2215 m elevation. Members 3 and 4 of the Miocene Altos de Pica Formation are exposed in this scarp (Fig. 5c). At the field site, Member 3 is 170 m thick and contains fluvial conglomerates and sandstones interbedded with aeolian deposits. Member 4 is a rhyolitic welded tuff that tapers westward from several hundred meters thick on the Altos de Pica plateau to zero above the 2000 m contour, east of Pica. We measured its strongly welded base at 29 and 47 m thick in two locations, whereas the member is weaker (Dingman and Galli, 1965) and more fluvially dissected up-section. It is porphyritic, 45–85% groundmass, and mostly medium to very hard. The Geologic Map of Chile from the Servicio Nacional de Geología y Minería (2003) describes the tuff as part of a lower–middle Miocene dacitic to rhyolitic pyroclastic sequence associated with collapsed calderas.

In summary, Miocene ignimbrites (including welded tuffs) cap the headscarps and directly overlie upper Oligocene to Miocene epiclastic strata at both field sites (Dingman and Galli, 1965;

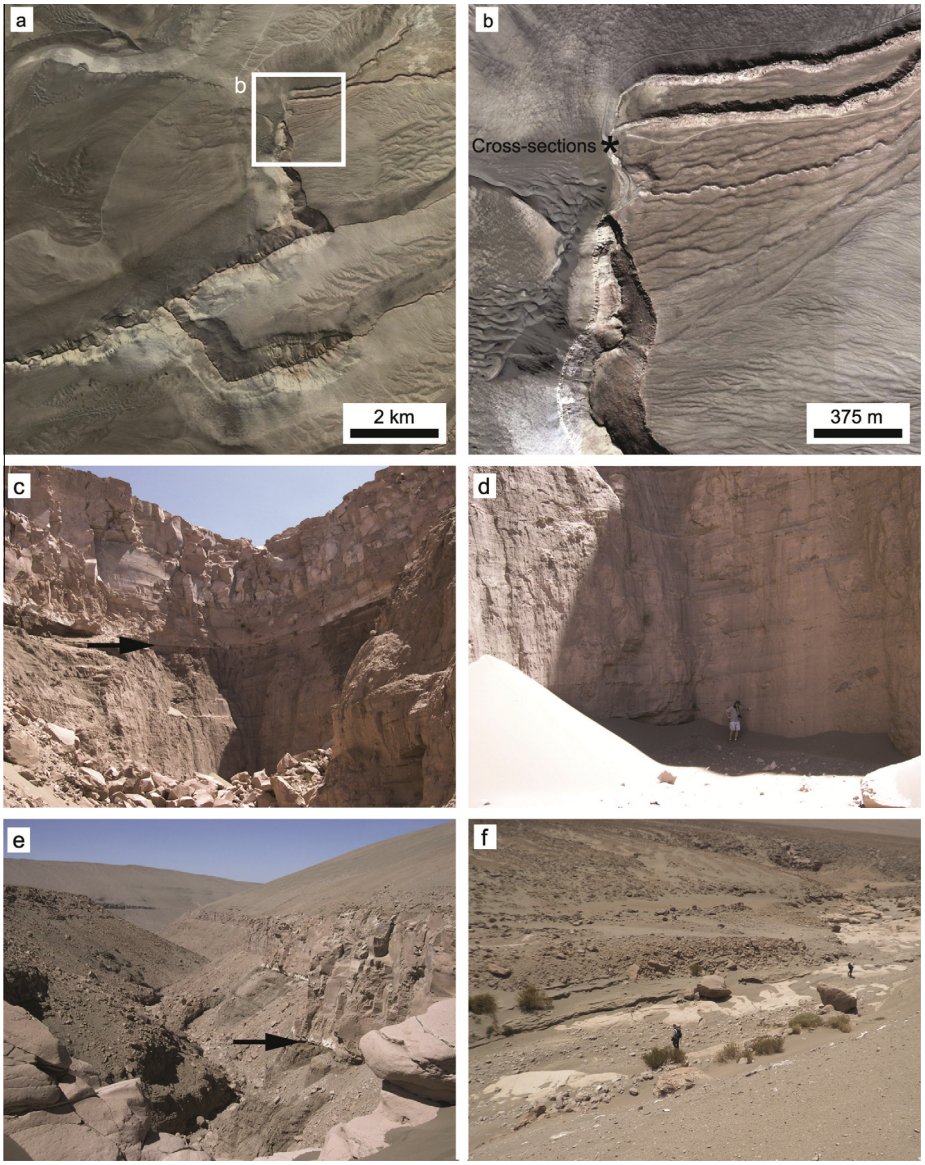

Fig. 5. Quebrada de Quisma. (a) Overview of headscarp area (Google Earth imagery), with area covered by (b) outlined. (b) Enlargement of headscarp (Google Earth imagery), with location of two measured channel cross sections labeled (both at this point, a short distance apart). (c) View of upper part of headscarp, with arrow indicating contact between welded tuff and underlying epiclastic strata. (d) View of base of headscarp. Note the lack of spring discharge, alcove development, or dense vegetation. Aeolian fill is visible on the valley floor and left side of the scene. (e) View downvalley from top of headscarp, with arrow indicating contact between welded tuff and underlying epiclastic strata. Note the steep scarp in the resistant tuff and the lower slope in the weaker underlying strata. (f) Mixed bedrock/gravel bed channel upvalley of headscarp (flow direction from left to right), at the location marked by * in (b).

García et al., 2004). Taken alone, the stratigraphy does not exclude any of the three major explanations for theater-headed valleys: groundwater sapping, flood erosion of strong-over-weak stratigraphy, or erosion of vertically jointed rock by larger floods (Section 1).

3. Methods

To determine whether a groundwater sapping origin for the Chilean quebradas can be confidently inferred from remote-sensing data alone, we evaluated this previous interpretation along with alternatives at the Quebradas de Humayani and Quisma. As we describe in the discussion section, one field site was not consistent with any of the processes indicated by earlier studies of theater-headed valleys, and we introduce landsliding as another possibility. Field data collection included: observations of the hydraulic, morphological, sedimentological, and vegetative features that are commonly associated with groundwater sapping; strength measurements of the strata exposed in the valley headscarps; and estimates of recent geomorphically effective flood discharges in the ephemeral channels. At the time of field work in March 2009 and January 2010, there were no active springs or relict spring-fed channels from which to take discharge measurements and to contrast with the estimates of flash flood discharges in the ephemeral channels.

3.1. Characteristic features

Recognizing an important role for groundwater sapping, flood erosion of strong-over-weak stratigraphy, or flood erosion of vertically jointed rock begins with a list of diagnostic characteristics, based on idealized process-form relationships outlined in the earlier publications cited below. For the purpose of this study, we were limited to small-scale characteristics that are observable in

the field, because relationships between form and process as seen in remote-sensing data (e.g., plan view morphologies and topography observed by satellites) are the subject of the investigation.

Within the context of groundwater sapping, characteristic features of active seepage weathering commonly (but do not necessarily) include overhanging alcoves with active springs, vegetation watered by the springs, and salt-weathered alcove surfaces that partly surround the wet areas. An aquifer overlying an aquiclude, with the contact exposed near the base of the headscarp, could concentrate spring discharge (e.g., Laity and Malin, 1985). In these situations, the cross section near the valley head is commonly rectangular to trapezoidal. The flat floor of this cross section is much wider than any ephemeral waterfall that flows over the headscarp, such that abrasion, plucking, and spray resulting from surface flooding are ineffective weathering and erosional agents for most of the width of the headscarp. (For many martian examples, the trapezoidal cross section may be a secondary feature resulting from mass wasting and aeolian infilling of ancient valleys rather than the primary morphology described here (Williams and Phillips, 2001).) Identifying dominant seepage erosion is straightforward, as the downstream channel dimensions and transported particle sizes should be consistent with measured spring discharges rather than much larger surface floods generated by precipitation.

In contrast, waterfalls can attack the entire narrow base of a headscarp in theater-headed valleys with a narrow or V-shaped cross section near the head (e.g., Fig. 5e). Haviv et al. (2010) describe the physical processes that operate at waterfalls. A V-shaped cross-sectional morphology may reflect active downcutting in weaker strata that cannot maintain vertical sidewalls, or it could imply more active weathering and slope processes. For both trapezoidal and V-shaped cross sections, the stream does not directly attack the upper part and flanks of the headscarp, which retreat mostly through mass wasting. These slope failures result in a rounded (theater-shaped) headscarp planform and a valley that is considerably wider than the stream. The waterfall attacks the base of the headscarp, facilitating its faster retreat relative to the sidewalls. In an end-member model dominated by flood erosion at waterfalls rather than groundwater sapping, the headscarp base is not much wider than the waterfall in flood and may lack evidence for enhanced weathering (e.g., Lamb et al., 2007).

In addition to groundwater sapping and basal attack by waterfalls, a third mechanism for headscarp retreat is toppling of columns in vertically jointed rock by surface floods that cascade over the headscarp (Lamb and Dietrich, 2009; Lamb et al., 2014). This process could occur independently of enhanced weathering or lithologic weakness at the base of the headscarp, providing that the jointing is continuous and dips nearly vertically. A basal detachment is also assumed. This configuration facilitates headscarp retreat as shear and drag during floods topple the jointed columns and remove the resulting debris. This process is also not expected to yield valley floors that are much wider than the stream, unless the valley was carved by a past flood that was much larger than the present stream (e.g., Lamb et al., 2008a, 2014).

3.2. Strength measurements

As described in Section 2.2, the study sites are characterized by strong-over-weak stratigraphy. To evaluate the relative resistance of overlying and underlying lithologies to weathering and fluvial erosional processes, we measured the compressive strength of exposures in the headscarps using a N-type Schmidt hammer, and we used the Selby (1980) classification to evaluate the rock mass strength. This combination of common field methods provides strength measurements from the centimeter scale up to the height of the outcrop.

Following convention (e.g., Selby, 1993), Schmidt hammer measurements were taken on relatively smooth rock surfaces >6 cm from an edge or joint. Loose particles were abraded from the surface using a carborundum tool, and the surface was measured (impacted) multiple times, with each measurement taken at least a plunger diameter from the previous one. The rebound value (R value) was recorded for each measurement, with a note on whether the hammer was held horizontally or vertically down.

The literature contains a variety of recommendations for how Schmidt hammer R value data should be reported. For example, the International Society for Rock Mechanics (1978) recommended 20 measurements and averaging the top 10. Katz et al. (2000) used 32–40 measurements and averaged the upper 50%. Selby (1993) recommended 20–50 measurements on each sample area of 2 m^2, then discarding the lower 20%, and continuing measurements until the deviation of the remaining ones from the mean is <3 points. Matthews and Shakesby (1984) took 15 measurements and discarded the five that deviated most from the mean. The Proceq manufacturer instructions for the Schmidt hammer suggest taking 8–10 values and neglecting "values which are too high or too low (the highest and lowest values) in your calculation of the average value."

Schmidt hammer measurements are very sensitive to hair-line fractures, weathering, and other small weaknesses hidden beneath the surface of exposures, all of which could result in some low values that do not reflect the compressive strength of intact outcrop. To compensate for these finite variations, which would be more important in weathered than unweathered lithologies, we collected 30 measurements from each sample area of approximately 0.25 m^2 and then averaged the highest 50% to determine the R value. The compressive strength (N/mm^2) based on the R value is given by the manufacturer's table, which takes into account whether the instrument was held horizontally, vertically up, or vertically down.

We collected Schmidt R value measurements of the caprock at five locations in the Quebrada de Humayani and at three locations in the Quebrada de Quisma. In the underlying epiclastic strata (e.g., Fig. 6), we collected measurements at five locations in the former site and at four locations in the latter.

At these locations, we also noted jointing and other bulk rock characteristics that contribute to the Selby (1980) rock mass strength classification. These factors include the intact rock strength based on the Schmidt R value (20 points maximum in the Selby scheme), weathering (10), joint spacing (30), joint orientations (20), joint width (7), joint continuity (7), and outflow of groundwater (6), for a maximum total of 100 points. We characterized these factors as described by Selby (1993, pp. 94–101). Rocks are then classified as very strong (100–91 points), strong (90–71), moderate (70–51), weak (50–26), and very weak (<26). The Selby (1980) rock mass strength is related to equilibrium slope as described by Abrahams and Parsons (1987) and Selby (1993). For example, vertical slopes can be maintained in strata with a rock mass strength of ~78–93, whereas the range of mass strength for 45° slopes is ~60–80. These estimates are approximate, because as Selby (1993) noted, other factors such as buttressing can affect actual slope values. Headscarps observed in the field were not buttressed, but the arched planform of the headwall adds to its strength as discussed below.

3.3. Discharge and runoff production

Precise flow measurements are not available for the ephemeral streams described here, but order-of-magnitude estimates provide a reasonable and quantitative constraint on flow and thresholds of motion in the hyperarid Atacama Desert. At the study sites, we estimated the discharge Q (m^3/s) of past flash floods in ephemeral

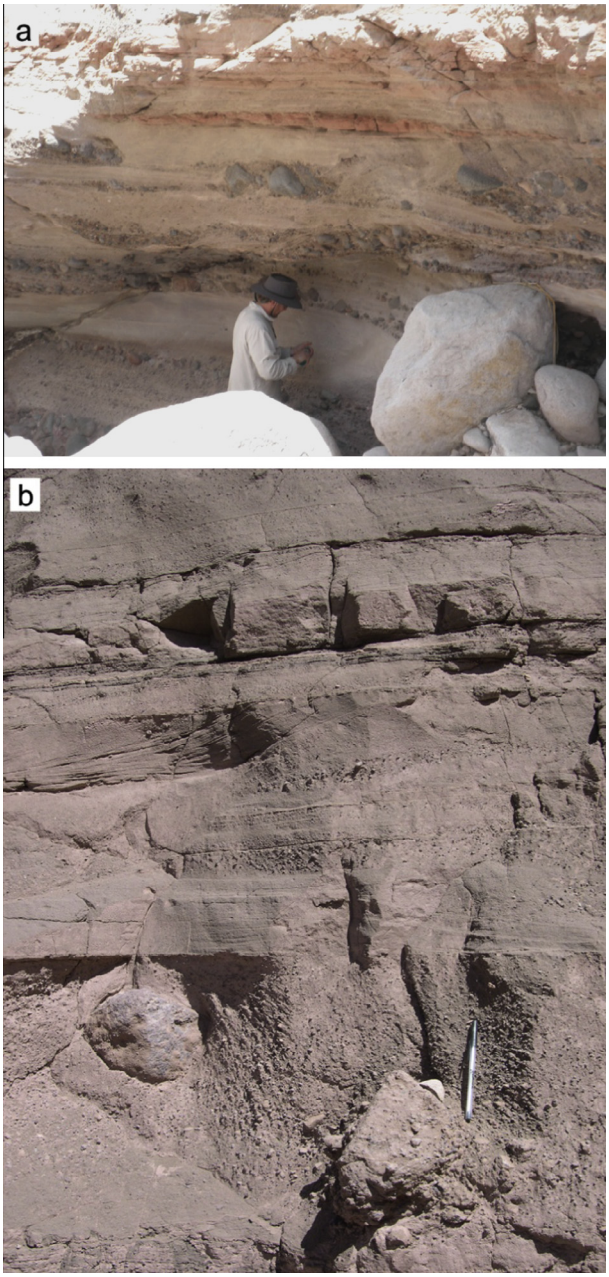

Fig. 6. Example outcrops of epiclastic strata exposed beneath welded tuff caprocks. (a) Quebrada de Humayani, north wall, west and down-section of outcrop shown in Fig. 4d. (b) Quebrada de Quisma, west wall, near base of headscarp shown in Fig. 5. In (a), note that transported boulders have larger grain size than eroded conglomerates.

channels upstream of the headscarps using the continuity (Eq. (1)) and Manning (Eq. (2)) equations

$$Q = AV \tag{1}$$

$$V = R^{2/3}S^{1/2}/n \tag{2}$$

In Eqs. (1) and (2), A is the cross-sectional area of the stream (m^2), V is mean velocity (m/s), R is the hydraulic radius (cross-sectional area divided by wetted perimeter, m), S is slope (m/m), and n is the Manning roughness coefficient ($s/m^{1/3}$). As recommended by Lumbroso and Gaume (2012), to ensure that our discharge estimates represent subcritical flow, we checked to see that the Froude number, Fr:

$$Fr = V/(gH)^{0.5} \tag{3}$$

was <1, where g is gravitational acceleration (9.81 m/s^2), and R is substituted for depth H (m). R is similar to mean channel depth.

We selected two measurement sites, one in a tributary within the Quebrada de Humayani (Fig. 4c) and one in the Quebrada de Quisma (Fig. 5b), both of which minimized complexity in the cross section and had well-developed recent high-water marks on alluvial banks (i.e., bilateral benches of transported debris or sediment). In the Quebrada de Humayani, the master (trunk) stream had a bed of rounded boulders with a range of diameters up to 2 m (Figs. 4d and 6a), potentially transported from a watershed of 305 km^2, although some of the largest boulders may have been locally derived from rockfall and abraded more or less in place. The roughness and irregularity of the master stream bed reduced confidence in a discharge estimate there, whereas the tributary provided a more reliable estimate of geomorphically effective discharge and runoff production.

At each measurement site, we obtained two cross-sectional profiles by stretching and leveling a measuring tape between opposite banks at the elevation of recent high-water marks and measuring the depth at major breaks in cross-sectional slope across the channel (typically ~10 depth measurements per cross section) (Fig. 7). We used high-water marks for recent floods rather than the maximum possible stream depth, so the calculations provide minimum discharge estimates for channels that may have experienced higher peak floods in the past. We calculated A and R from the cross-sectional profiles. We measured S between the two cross sections

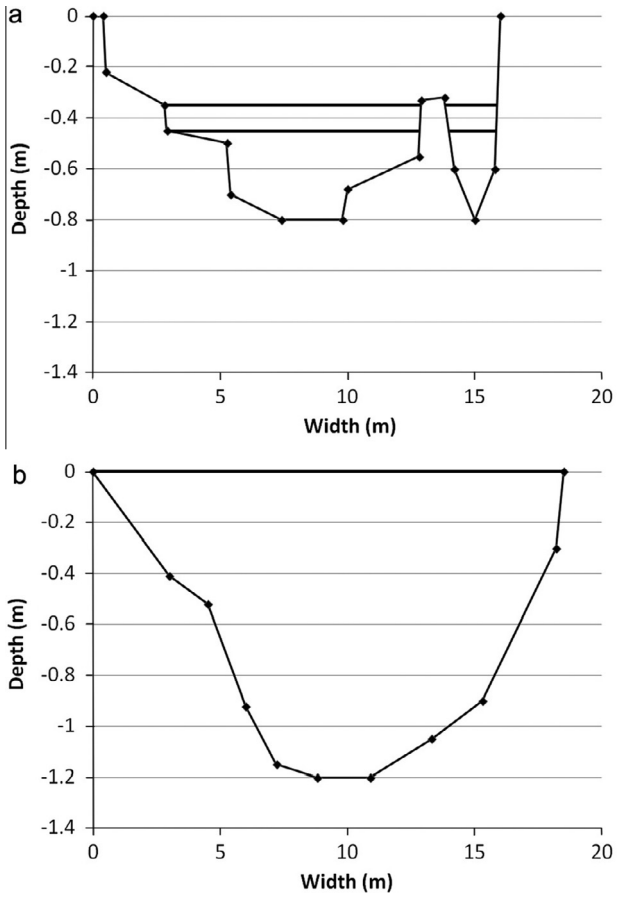

Fig. 7. Channel cross sections of (a) a tributary to the Quebrada de Humayani and (b) the Quebrada de Quisma. The horizontal lines show inferred water surface elevations as discussed in the text. The flow direction is out of the page in both plots. Locations are shown in Figs. 4c and 5b, respectively.

using the inclinometer on a Laser Technology TruPulse 200 rangefinder, which has an accuracy of ±0.0044 or 0.25°. Manning's n was estimated in the field using the Barnes (1967) scheme, which allows a visual comparison between the observed channel bed and channels with known Manning's n. We also made tri-axial measurements (A, B, C axes) of the 20 largest transported (rounded and/or imbricated) gravel clasts in the stream bed and estimated the critical shear stress for transport, τ_c (N/m^2), using the Shields equation, assuming a Shields coefficient of 0.045, typical of hydraulically rough beds (Komar, 1988):

$$\tau_c = 0.045(\rho_s - \rho_w)gD \quad (4)$$

The variables ρ_s and ρ_w are the densities of sediment (mainly felsic, in this case) and water, respectively (~2650 and 1000 kg/m^3); and D is the grain diameter (m), for which we used the median intermediate (B) axis of the transported gravel clasts. Assuming steady and uniform flow, the bed shear stress τ is:

$$\tau = \rho_w gRS \quad (5)$$

In Eqs. (4) and (5), all of the variables except R are known or measured, so solving for R provides a critical hydraulic radius for transport. This value can be compared to the channel dimensions below high-water marks. We calculated a runoff production rate by dividing the calculated Q by the upstream contributing area A_c, with the latter measured from a georeferenced satellite image and then checked against the watershed area derived from Shuttle Radar Topography Mission data using Blue Marble Geographics Global Mapper 13 software.

The main sources of error in Eqs. (1)–(5) include: (1) for discharge calculations, selection of an appropriate Manning's n and accuracy of the inclinometer slope; and (2) for critical shear stress and flow depth for transport, the Shields coefficient (e.g., Lamb et al., 2008b), sediment density, and slope. To maintain a Froude number below unity, Manning's n could not have been less than about 0.07 in the Quebrada de Humayani tributary or 0.045 at the Quebrada de Quisma. The error in discharge associated with the slope measurement, based on the published instrument accuracy of ±0.0044 or 0.25°, is ±0.1 m^3/s (~3% of the Q estimate) at the Quebrada de Humayani tributary and ±4 m^3/s (~10% of Q) at the Quebrada de Quisma (see Section 4.3). A Manning's n value that yields Fr near unity would thus provide discharge and runoff production estimates that are near the maximum possible for the interpreted flood stages. The critical shear stress and depth for transport are directly proportional to the Shields coefficient. Andesite and rhyolite densities typically vary by ±10% relative to the 2650 kg/m^3 value that we used. The slope errors of ±0.25° would be ±6% of the measured slope at the Quebrada de Humayani tributary and ±25% at the Quebrada de Quisma, requiring proportionally deeper or shallower water to offset changes in slope and transport the measured clasts. Taking all of these sources of error into consideration, in order to test the geomorphic effectiveness of surface floods, the critical hydraulic radius for transport needs to be close to the measured R, but it does not need to be exactly the same.

4. Results

4.1. Characteristic features

The Quebrada de Humayani headscarp is characterized by steep (near-vertical) outcrops of the Oxaya Ignimbrite's welded tuff, with talus slopes below (Fig. 4b). The master ephemeral stream in the quebrada has dissected the headscarp, so the contact between the tuff caprock and the underlying strata is now exposed along the thalweg approximately 2 km upstream of the headscarp. In the study area, the master stream lacks significant vertical knickpoints, including where the trace of the headscarp crosses the stream. Sparse, shrubby vegetation is found along the master stream thalweg, but the surrounding slopes, the base of the headscarp, and locally sourced tributaries are barren. Spring discharge, salt-weathered alcoves, or areas of dense vegetation were not observed at the headscarp.

Below the headscarp, the floor of the Quebrada de Humayani is mapped as Pliocene–Quaternary mass wasting deposits. Specifically, these deposits are polymictic breccias with a variable sand/silt matrix, derived from gravitational sliding or avalanches (Servicio Nacional de Geología y Minería, 2003; García et al., 2004). Where not subsequently buried or dissected by the ephemeral drainage network, the primary morphology of these mass wasting deposits is preserved over the >2 km width of the valley floor (Fig. 4b).

At the Quebrada de Quisma, the headscarp is near vertical, and no talus has accumulated at its base (Fig. 5c and d). We observed no spring discharge, salt-weathered alcoves, or vegetation below the headscarp. Above the headscarp, however, sparse vegetation is present along the bed of the ephemeral stream (Fig. 5f), and plastic and other trash was embedded in sandy flood deposits, demonstrating that the stream is occasionally active even in the modern hyperarid climate. This stream unequivocally overspills the headscarp when it is active, with a discharge and sediment transport competence that are described below. The plunge pool area is mostly buried by sand (Fig. 5d), possibly derived from the active aeolian dune field on the adjacent western slope.

4.2. Strength measurements

Both of the theater-headed valleys studied in the field include ignimbrite caprocks (including resistant welded tuffs) over epiclastic strata. In the welded tuff within the Oxaya Ignimbrite at the Quebrada de Humayani, the compressive strength based on Schmidt hammer R values was >59 N/mm^2 at four out of five sites (Table 1). In contrast, an underlying pink submember of the Oxaya Ignimbrite returned three compressive strength values at <10, one at 15, and one at 27 N/mm^2. The highest compressive strength (27 N/mm^2) was measured in an unweathered, fluvially sculpted and polished chute, suggesting that the unweathered pink submember has moderate (albeit variable) strength, and that weathering reduces that strength. The underlying epiclastic rocks returned five compressive strength estimates ranging from 16 to 19 N/mm^2. These data suggest that the welded tuff has multiple times the compressive strength of the underlying strata.

In the Altos de Pica member 4 (welded tuff) at the Quebrada de Quisma, compressive strength was >60 at two sites and 38 N/mm^2 at another (Table 1). The latter site may represent a more weathered or less welded surface, but strength is still much higher than for the underlying epiclastic strata, which had compressive strengths of 14–17 N/mm^2.

The Schmidt hammer R values were also incorporated into the Selby (1980) rock mass strength values. Rock mass strength was 84 for the welded tuff and 73 for the underlying epiclastic strata at the Quebrada de Humayani, with similar figures of 84 and 64, respectively, at the Quebrada de Quisma (Table 2). Hence, the welded tuffs had a "strong" mass strength and should maintain vertical or near-vertical scarps, whereas the underlying epiclastic rocks were "moderate" to "strong", and lower-angle slopes should be more likely to develop (Abrahams and Parsons, 1987; Selby, 1993). These relationships are consistent with field observations; for example, as shown by the Quebrada de Quisma cross section (Fig. 5e). Joints were mostly continuous with fair (i.e., horizontal or nearly vertical) orientations.

Table 1
Schmidt hammer *R* values and corresponding compressive strength of caprock and underlying lithologies exposed in headscarps.

Quebrada, lithology	Schmidt hammer *R* value[a]	Compressive strength (N/mm^2)[b]
Humayani, welded tuff (caprock)	53 V	60
	46 H	43
	60 H	>60
	59 V	>60
	55 H	59
Humayani, pink ignimbrite (underlying)	19 H	<10
	17 H	<10
	15 H	<10
	35 H	27
	23 V	15
Humayani, epiclastic (underlying)	27 H	17
	30 H	19
	28 H	18
	28 H	18
	27 H	16
Quisma, welded tuff (caprock)	57 V	>60
	38 V	38
	62 H	>60
Quisma, epiclastic (underlying)	28 H	17
	25 H	14
	25 H	14
	25 H	14

[a] V is vertical hammer orientation (down), H is horizontal.
[b] The manufacturer's table relates *R* values to compressive strengths from 10 to 60 N/mm^2.

4.3. Discharge and runoff production

Using methods described in Section 3.3, we estimated the recent flash flood discharge for a tributary stream to the Quebrada de Humayani and for the master stream in the Quebrada de Quisma. The Quebrada de Humayani tributary (18.892749°S, 69.741445°W, Fig. 4c) had a thalweg depth of 0.35 m, hydraulic radius *R* of 0.21 m, slope *S* of 0.072, and Manning's *n* of approximately 0.07, yielding a velocity *V* of 1.3 m/s. The cross-sectional area *A* was 2.5 m^2, so the discharge estimate *Q* is approximately 3.3 m^3/s. This *Q* corresponds to runoff production of 1.5 cm/h from the drainage area A_c of about 0.825 km^2 during a rainfall event. The Froude number for this flow was 0.94. The 20 largest transported (rounded and/or imbricated) particles in the channel thalweg had a median *B* axis of 0.25 m, and the calculated critical hydraulic radius for transport was 0.26 m, which is slightly above the measured *R* at this stage. If the flow were 0.45 m deep at the thalweg (approximately critical at $Fr = 0.98$ and laterally confined in the cross section), then *R* is 0.26 m, *V* is 1.6 m/s, *A* is 3.6 m^2, *Q* is 5.7 m^3/s, and runoff production is 2.5 cm/h. Gravel- and coarser-bedded streams are commonly just above the critical conditions for transport at bankfull (e.g., Parker et al., 2007). Older, higher-standing channel bars contained coarser rounded particles, suggesting that this tributary watershed had generated more runoff at times in the past, although we judged the stage indicators to be less reliable and the cross section to be less well preserved than for the later flood reported here. The measurements were taken at 1990 m elevation, and the headwaters were at about 2230 m, 1.5 km to the northeast. Many of the transported clasts were reworked from a bouldery alluvial deposit that caps this northern drainage divide, rather than derived from local bedrock.

The master stream in the Quebrada de Quisma (20.47°S, 69.185°W, Fig. 5f) had a mixed bedrock/gravel bed with well-defined erosional and depositional paleostage indicators. For these levels at one cross section, we found *R* of 0.77 m, *S* of 0.018, and *n* of approximately 0.05, yielding *V* of 2.2 m/s. *A* was 14.5 m^2, giving a *Q* of 32 m^3/s. This discharge would represent runoff production of 0.1 cm/h from the watershed of 116 km^2. At a second cross section downstream, *R* was 1.0 m, and we used the same *S* and *n*, giving *V* of 2.7 m/s. *A* was 14.9 m^2, and the *Q* estimate was 40 m^3/s, representing runoff production of 0.13 cm/h from the watershed. Larger watersheds such as this one typically experience spatially non-uniform runoff production during storms, which may account in large part for the lower runoff production relative to the smaller tributary described above. The hanging, locally sourced tributaries to the Quebrada de Quisma suggest that most of the runoff originates higher in the Andes, well above the 2238 m elevation of the channel cross sections. The Froude numbers (*Fr*) at the upper and lower cross sections were 0.81 and 0.85, respectively. The median *B* axis of 20 rounded and/or imbricated particles was 0.39 m, requiring 1.6 m as the critical hydraulic radius for transport. The channel depth below the paleostage indicators was 1.2–1.5 m, and *R* was 0.77–1.0, respectively, suggesting that floods above these indicators were responsible for transport of the clasts.

Literature on the Quebrada de Chacarilla, which shares part of its drainage divide with the Quebrada de Quisma (Fig. 3b), provides a consistent estimate of runoff production in that area. At the Quebrada de Chacarilla, a low north–south ridge collects drainage from an area 60 km across between 3500 and ~4300 m elevations, and this water is funneled through a gap in the ridge into the main

Table 2
Selby rock mass strength data (score for each parameter is given in parentheses).

Parameter	Humayani, welded tuff	Humayani, pink ignimbrite	Humayani, epiclastic	Quisma, welded tuff	Quisma, epiclastic
Schmidt hammer *R* value[a]	60–50	35–10	35–10	60–50	35–10
	(18)	(5)	(5)	(18)	(5)
Weathering	Slightly	Moderately	Slightly	Slightly	Slightly
	(9)	(7)	(9)	(9)	(9)
Joint spacing	1–3 m	1–3 m	1–3 m	1–3 m	1–0.3 m
	(28)	(28)	(28)	(28)	(21)
Joint orientation	Fair	Fair	Fair	Fair	Fair
	(14)	(14)	(14)	(14)	(14)
Joint width	1–5 mm	1–5 mm	1–5 mm	5–20 mm	1–5 mm
	(5)	(5)	(5)	(4)	(5)
Joint continuity	Continuous, thin infill	Continuous, thin infill	Few continuous	Continuous, no infill	Continuous, thin infill
	(4)	(4)	(6)	(5)	(4)
Groundwater flow	None	None	None	None	None
	(6)	(6)	(6)	(6)	(6)
Total rating	(84)	(69)	(73)	(84)	(64)
	Strong	Moderate	Strong	Strong	Moderate

[a] The mean *R* value from multiple measurement sites falls into this range as used in the Selby (1993) scheme.

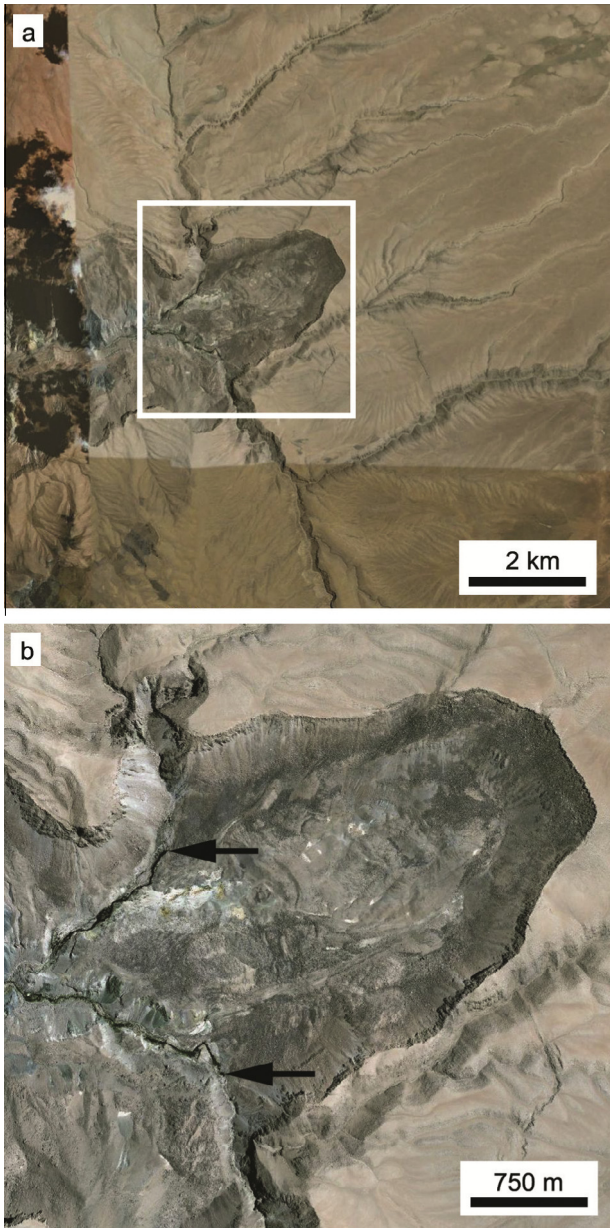

Fig. 8. Quebrada de Chacarilla. (a) Overview of headscarp and surrounding area (Google Earth imagery), with area covered by Fig. 8b outlined. Note that the headscarp has advanced up a drainage divide rather than tracking along the largest contributing surface ephemeral streams. (b) Enlargement of headscarp (Google Earth imagery), showing increased vegetation density in channel reaches indicated by arrows. Note the lack of fluvial dissection between the headscarp and points where tributaries enter from the north and south.

east–west-trending valley (Figs. 3b and 8). Houston (2001, 2002) published a discharge estimate of $450 \pm 50\ m^3/s$ from the 1235 km^2 Chacarilla watershed for a flash flood in January, 2000. The runoff production was 0.13 cm/h. The storm produced 34 million m^3 of runoff, about 70% of which infiltrated into the alluvial fan where the quebrada debouches to the Pampa del Tamarugal. The return period was estimated at four years (Houston, 2001, 2002).

5. Discussion

These field data are useful for evaluating the possible hypotheses for theater-headed valleys outlined in Section 1: groundwater sapping, flood erosion of strong-over-weak stratigraphy, and toppling of vertically jointed rock by floods. The mapping by García et al. (2004) also suggests a fourth hypothesis, that some larger theater-shaped headscarps in the region could be scars from large mass movements. A distinction is also possible between the physical processes that form a headscarp and the processes or rock characteristics that maintain it.

5.1. Groundwater sapping

At the two headscarps that we visited in the field, we observed none of the features that are commonly (but not necessarily) associated with groundwater sapping: spring discharge, salt weathering, alcoves, or areas of dense vegetation). Although we cannot exclude the possibility that these two valley headscarps originally formed by groundwater sapping (e.g., under past wetter conditions when increased runoff from the high Andes supported aquifer recharge), seepage weathering and seepage erosion do not appear to be actively maintaining or developing these headscarps in the present hyperarid climate.

At the Quebrada de Humayani, the master stream has fully dissected the headscarp, and it and its tributaries have also incised extensive mass wasting deposits below the scarp (Fig. 4) (García et al., 2004). Away from the incising channels, younger talus has buried the base of the headscarp (Fig. 4b), suggesting that undercutting of the scarp has either stopped or is now slower than the production of talus. These observations suggest that the process or processes that initially formed the Humayani headscarp are not actively developing it at present.

In contrast, the Quebrada de Quisma headscarp is vertical, and no talus has accumulated at its base (Fig. 5d). Although talus is present along the sidewalls downstream (Fig. 5e), the headscarp appears to be actively maintained, but by processes other than groundwater sapping.

5.2. Flood erosion of strong-over-weak stratigraphy

The slope of initially vertical knickpoints tends to decline over time in homogeneous, cohesive material, but vertical knickpoint faces can be maintained during retreat by certain stratigraphic, structural, or undermining (sapping) factors (Gardner, 1983). Strong-over-weak stratigraphy can support retreat of vertical knickpoints through erosion at waterfalls, and both the Quebrada de Humayani and Quebrada de Quisma sites have resistant Miocene ignimbrite caprocks (including welded tuffs) overlying weaker epiclastic strata. At both sites, compressive strengths for the caprocks can be over 60 N/mm^2, multiple times the values for the underlying strata (Table 1). With Selby (1980) rock mass strength values over 80 (Table 2), the caprocks should be able to support vertical or near-vertical scarps, whereas the underlying strata should not. This differential strength may lead to headscarp retreat by undercutting of the caprock during floods, collapse of the caprock, and flood transport of the resulting debris.

The cross section of the Quebrada de Quisma is V-shaped downstream of the headscarp (Fig. 5e), consistent with the tendency of the weaker epiclastic strata to develop sub-vertical slopes. This shape also makes the entire narrow base of the headscarp susceptible to attack by a waterfall. Sizeable ephemeral floods from an overland channel (Fig. 5a and b) overtop that headscarp, transport coarse sediment, and erode the channel bed, thus demonstrating the ability to erode the headscarp at a waterfall. The Quebrada de Quisma stream and Quebrada de Humayani tributary have flood discharges of cubic meters to tens of cubic meters per second and transport clasts up to tens of centimeters in diameter, making them effective at attacking the underlying strata through abrasion and plucking. Moreover, the clast size of epiclastic strata exposed

at the base of the scarps in both the Humayani and Quisma sites was less than the clast size transported in the modern streams (Fig. 6), implying that these strata can break down to transportable sizes. Upstream of the headscarp, parts of the Quisma stream bed are fluvially sculpted in welded tuff (Fig. 9), further demonstrating the erosional impacts of flash floods. Our estimates of flood discharge and runoff production are three orders of magnitude higher than any reasonable spring flow.

The ignimbrite that comprises Member 4 of the Altos de Pica Formation pinches out between the study site and Pica (located downstream of the Quisma headscarp), so an independent scarp-forming process (other than erosion by surface floods) was not needed to expose the edge of the resistant unit. Therefore, flood erosion of strong-over-weak stratigraphy could have both formed and maintained the Quebrada de Quisma headscarp, although we cannot interpret the original formation processes with as much confidence as the current maintenance processes.

Although strong-over-weak stratigraphy is also found at the Quebrada de Humayani headscarp, its 3 km width is difficult to explain through erosion by flash floods alone. Dense fluvial dissection of the underlying strata could promote slope retreat and undermining of the welded tuff caprock, but currently the valley floor is not densely dissected below the headscarp. For these reasons, strong-over-weak stratigraphy may help to maintain the Humayani headscarp against subsequent degradation, but it is likely not responsible for initially forming the scarp.

5.3. Flood erosion of vertically jointed rock

At both the Quebrada de Humayani and Quebrada de Quisma sites, continuous vertical jointing with typical horizontal joint spacing of a meter or more was observed in the welded tuff caprocks (Table 2). Upstream of the headscarp at both sites, ephemeral streams had incised the ignimbrites by meters to >10 m, forming sculpted surfaces in the welded tuffs (Fig. 9). At the Quisma site, the channel morphology changes significantly where the stream flows over the headscarp caprock and is able to attack the underlying strata. Erosion of the underlying rock is rapid, leading to undercutting of the tuff, which retreats by separation along joints and consequent rockfalls. The valley thus develops a much larger, V-shaped cross section with side slopes partly armored by tuff talus (Fig. 5). The arched shape of the headscarp in plan view maximizes strength against further slope failure and headward retreat, in much the same way that the shape of an arch dam adds to its strength. We interpret vertical jointing as a contributing factor to the ongoing retreat of the Quebrada de Quisma headscarp, but the fact that the headscarp exposes strong-over-weak stratigraphy suggests that jointing is not the sole cause.

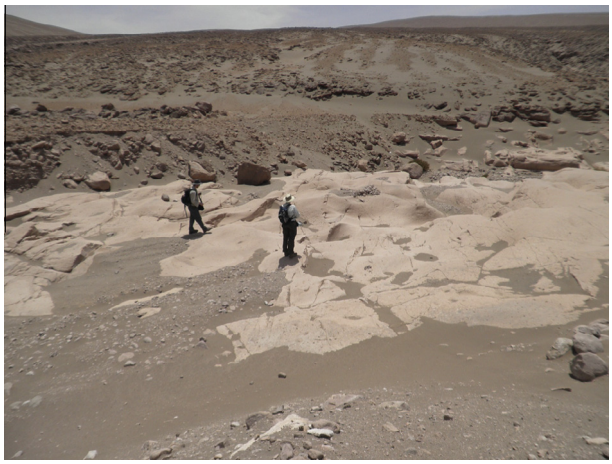

Fig. 9. Fluvially sculpted channel floor in welded tuff above Quebrada de Quisma headscarp, flow direction is from the left to the right.

5.4. Landslides

The Quebrada de Humayani floor contains extensive mass wasting deposits (García et al., 2004), which still maintain much of their original morphology (Fig. 4b). This observation, coupled with the 3 km width of the headscarp and the inadequacy of the master stream to attack and undermine the full width, suggests that the headscarp may be a scar from a giant landslide, maintained against later degradation by the strong welded tuff caprock. The base of this headscarp is not clearly exposed, now being widely buried by talus in areas away from the master stream. Although a wide valley floor covered by mass movement deposits is not conclusive evidence that the adjacent headscarp is a landslide scar, and past groundwater sapping is not excluded, landsliding is the only explanation for which we have found supporting evidence.

Giant landslides have been reported from other parts of the Atacama Desert, including on the western slope of the Chilean Andes <70 km to the north and south of the Quebrada de Humayani (Strasser and Schlunegger, 2005; Pinto et al., 2008). Strasser and Schlunegger (2005) speculated that important contributing factors for the giant Lluta landslide to the north may have been: (1) cohesive strength along the basal shear plane; (2) a weak detachment horizon at the top of the Azapa Formation; (3) an elevated groundwater table that fluidized the basal shear zone; (4) pre-existing joints in the Oxaya Formation ignimbrites; (5) the steep dip of the strata; (6) incision of the Quebrada de Lluta near the eventual toe of the landslide; and (7) seismic activity. Any or all of these factors may also have contributed to the Quebrada de Humayani landslide or to others in the region. Pinto et al. (2008) interpreted a seismic trigger for the Latagualla landslide to the south, facilitated by its proximity to an active fault and possibly by a shallow water table. There may have been a groundwater influence on the morphology of the Latagualla study area, supported by other factors listed in this section, even if groundwater sapping in the strict sense (see Section 1) was not significant.

The Quebrada de Humayani has some morphological similarity to the Quebrada de Chacarilla, which was also studied remotely by Hoke et al. (2004) and attributed to groundwater sapping. At the Quebrada de Chacarilla headscarp (Fig. 8), which we were unable to visit due to limited accessibility, a lower–middle Miocene ignimbrite caprock overlies continental mudstone, shale, sandstone, and lava of the Jurassic Chacarilla Formation, as well as Cretaceous trachyte and breccia (Servicio Nacional de Geología y Minería, 2003). The headscarp is about 1.5 km wide and 150–200 m high, with the top of the scarp at ~3550–3725 m elevation. Similar to the Humayani headscarp, the base of the Chacarilla scarp is covered by a talus slope, and a rolling surface with blocky deposits characterizes the valley floor below the headscarp (Fig. 8b). Unlike the Humayani headscarp, however, the Chacarilla headscarp has advanced up a low divide that separates the two major tributary watersheds (Quebrada Chara from the north and northeast, and Quebrada Caya from the south and southeast, Fig. 8a). Dense vegetation occurs in the thalwegs of these two streams at about 3270–3280 m elevation, 200 m below and 1.8–2 km southwest of the point where the headscarp base meets the valley centerline, and perennial flow is maintained in the upper reach of the Quebrada de Chacarilla (Houston, 2002). In orbital imaging, however, we see no evidence for spring discharge or dense vegetation at or near the headscarp itself (Fig. 8b). The location of the headscarp on the drainage divide between two tributary streams is uncommon for theater-headed valleys, and together with the rolling, little-dissected relief below the headscarp, it may be more

consistent with giant landsliding than with a fluvial origin. A role for groundwater-facilitated landsliding in forming this headscarp is also possible, particularly under wetter conditions in the past (e.g., Quade et al., 2008; Gayo et al., 2012). The headscarp is clearly not developing as a result of flash flood erosion in ephemeral streams, and strong-over-weak stratigraphy may limit its degradation, as with the Quebrada de Humayani.

6. Implications for interpretation of Mars

Based largely on remote-sensing data and publications, Hoke et al. (2004) presented a reasonable argument for a groundwater sapping origin of three theater-headed valleys in northern Chile. Although the available data do not exclude groundwater sapping at these sites in the distant past, our field observations at two of these sites are more consistent with alternative hypotheses. The Quebrada de Quisma headscarp may have originated as, and is continuing to develop by, flood erosion of strong-over-weak stratigraphy, facilitated by vertical jointing in the welded tuff caprock. The Quebrada de Humayani headscarp appears to be a scar produced during a giant landslide within the valley. The Quebrada de Chacarilla headscarp may also have originated as a scar from a giant landslide, but from this location we have no field data with which to comment more definitively.

We thus maintain that the dominant diagnostic features of groundwater sapping that Hoke et al. (2004) reported in this study area (see Section 1) are not diagnostic of that process. The depth of the quebradas is a response to dissection of the coastal escarpment (Fig. 3a), the headwalls are either landslide scars or an erosional response to strong-over-weak stratigraphy, and springs occur elsewhere along the western slope but not at the canyon headwalls. The quebradas are only nonbifurcating along their lower reaches, which do not generate significant runoff, whereas the headwater areas in the Andes are quite densely dissected (Figs. 2 and 3).

Our observations also present a cautionary tale for investigations of theater-headed valleys on Mars, where surface observations are not yet widely available. Parts of Mars may have strong-over-weak stratigraphy due to volcanism or cementation of surface materials (Jakosky and Christensen, 1986; Howard et al., 2005; Craddock et al., 2012). Vertical jointing of surficial materials is also possible. Measurements of fluvial channels on Mars suggest significant discharges and runoff production rates, at least intermittently (Irwin et al., 2005). The role of landslides in the development of some theater-headed valleys, particularly those with wide headscarps and relatively flat floors as opposed to V-shaped cross sections, is worthy of future work. These alternative hypotheses should be considered when interpreting theater-headed valleys, which should not be attributed by default to groundwater sapping on the basis of planform morphology alone. Secondary infilling of the valley after flow ceased should also be considered when attempting to explain the development of flat valley floors on Mars (Williams and Phillips, 2001).

Depending on the depth of a valley, the weakness of the rock into which it is incised, and the effectiveness of slope processes (which control the slope gradient), theater-headed valleys can develop a V-shaped cross section just downstream of the headscarp, such that the valley top width is much wider than the stream. Erosion is then focused in a narrow area at the base of the headscarp, such as near a waterfall plunge pool, as it is at the Quebrada de Quisma. The top and flanks of the headscarp as well as the valley sidewalls (areas not directly affected by the stream) retreat primarily through mass wasting, which is not limited by stream width. A wide theater headscarp above a wide, flat valley floor is likely not attributable to a single waterfall, but our observations suggest that equally it may not be a unique indicator of groundwater sapping.

Numerical models (e.g., Pelletier and Baker, 2011) indicate a positive relationship between discharge and erosion rate in the development of theater-headed valleys, but that relationship has only been demonstrated empirically in loose sand, not in bedrock (e.g., Howard and McLane, 1988; Perron and Hamon, 2012; Marra et al., 2014). These models do not include strong-over-weak stratigraphy, vertically jointed rock, or the physics of waterfalls. Without incorporating these physical influences on stream erosion (e.g., Haviv et al., 2010), the models can only produce theater-headed valleys from groundwater sapping, and they cannot be used to discriminate between groundwater sapping and surface flood erosion hypotheses for the formation of such valleys.

7. Conclusions

Based on remotely sensed imagery and topography, as well as publications on the local geology and hydrology, Hoke et al. (2004) had attributed three theater-headed valleys in the hyperarid Atacama Desert of northern Chile to groundwater sapping (Fig. 3). We used field data from two of these valleys (observation of characteristic features, strength measurements of strata exposed in headscarps, and discharge estimates) along with remotely sensed images and published geological information to evaluate three commonly cited hypotheses for theater-headed valleys: groundwater sapping, flood erosion of strong-over-weak stratigraphy, and toppling of vertically jointed rock by floods. We also identify landslides as a possible formative process for some large valley headscarps.

All of the headscarps illustrated by Hoke et al. (2004) have strong capping layers of Miocene ignimbrites overlying weaker epiclastic or other sedimentary strata (e.g., Fig. 5c), which are more susceptible to fluvial erosion. Some welded tuffs measured at our two field sites have a compressive strength of 60 N/mm^2 or more, multiple times that of the underlying strata (Table 1). The Quebrada de Quisma headscarp is vertical and lacks debris at the base (Fig. 5d), so it appears to be actively maintained under present hyperarid conditions. The Quebrada de Humayani headscarp has an exposed capping layer of welded tuff and a talus slope below it, but away from the master stream, little fluvial erosion is evident at the base of the headscarp (Fig. 4b), suggesting that the scarp-forming process is presently inactive at this site.

We estimated recent flood discharge at the Quebrada de Quisma and at a tributary within the Quebrada de Humayani. At Humayani, the master ephemeral stream had transported rounded boulders up to 2 m in diameter (Fig. 4d), and the very irregular channel bed reduced confidence in the cross-sectional geometry needed for a discharge estimate. The Quebrada de Quisma master stream had a discharge of 32–40 m^3/s, corresponding to runoff production of ~0.1 cm/h from the watershed of 116 km^2 during a flood. This runoff production was similar to a published estimate from the adjacent Quebrada de Chacarilla watershed of 1235 km^2 (Houston, 2002). The Quebrada de Humayani tributary had a discharge of approximately 3.3 m^3/s, or a runoff production of 1.5 cm/h from the much smaller drainage area of about 0.825 km^2. Both the Humayani and Quisma floods generated bed shear stresses adequate to transport gravel clasts with an intermediate axis of a few tens of centimeters, consistent with the size of rounded, imbricated clasts within the channels. These transported clasts were larger than the grain size of the deeply dissected epiclastic rocks beneath the welded tuff caprocks. Thus, ephemeral floods are capable of eroding these valleys in the current hyperarid environment, even at elevations as low as 2000 m in the Atacama Desert. In contrast, the large grain size and lack of spring discharge

at these two headscarps showed that seepage erosion (groundwater-derived base flow) is not responsible for sediment transport.

The headscarps visited in the field lacked spring discharge, salt weathering, alcoves, or vegetation, thus we found no evidence that groundwater sapping is actively maintaining the scarps. Our results suggest instead that the vertical headscarp at the Quebrada de Quisma may have originated by, and is currently maintained by, flood erosion of strong-over-weak stratigraphy, facilitated by continuous vertical jointing in the welded tuff caprock. The upstream channel conveys large discharges, transports coarse sediment, has a fluvially abraded channel floor, and drains over the headscarp; it is therefore capable of attacking the headscarp above, at, and below a waterfall. In contrast, the headscarp in the Quebrada de Humayani is 3 km wide, so it is unlikely to have originated by fluvial erosion at a narrow waterfall. Although we cannot exclude the possible influence of past groundwater sapping, our observations suggest that this headscarp may be a scar from a giant landslide, the debris of which still covers the valley floor below the scarp (García et al., 2004). Strong-over-weak stratigraphy helps to maintain this headscarp against subsequent degradation in areas away from the master stream.

This work suggests that deeply incised valleys with theater headscarps should not be attributed by default to groundwater sapping, as other processes may be responsible. This study reaffirms the importance of strong-over-weak stratigraphy and vertical jointing in the development of some theater headscarps (e.g., Lamb et al., 2006, 2008a), but it also suggests that the role of mass wasting (particularly in the form of giant landslides) in some cases may not be fully appreciated and is worthy of future investigation.

Particularly when referring to Mars, we prefer the term "theater-headed valley" over "sapping valley", because the latter is usually interpreted to imply groundwater activity, yet theater-headed martian valleys may not be the consequence of groundwater sapping. This study and other recent papers on terrestrial theater-headed valleys that specifically address the application to Mars (Lamb et al., 2006, 2007, 2008a) show examples where erosion at waterfalls and in vertically jointed rock can be responsible for headward retreat of vertical scarps. Below the headscarp, these terrestrial valleys tend to be narrow at the base, and wide, deep ones are V-shaped in cross section. We also note that primary mass wasting and secondary aeolian infilling can explain some theater-headed valleys with flatter floors near the headscarp, so cross-sectional geometry similarly may not be diagnostic without supporting field observations.

Acknowledgments

The NASA Mars Fundamental Research Program funded this study through Grants NNX07AV46G and NNX13AF10G (Smithsonian Institution). The sponsor had no role in the study methodology; collection, analysis and interpretation of data; writing of the paper; or in the decision to submit the article for publication. RPI completed some of this work while working as a visiting scientist at NASA Goddard Space Flight Center, Greenbelt, Maryland. We are grateful to Joel Johnson and an anonymous reviewer for their insightful, constructive comments on the manuscript.

References

Abrahams, A.D., Parsons, A.J., 1987. Identification of strength equilibrium rock slopes: Further statistical considerations. Earth Surf. Process. Landforms 12, 631–635.

Alpers, C.N., Brimhall, G.H., 1988. Middle Miocene climatic change in the Atacama Desert, northern Chile: Evidence from supergene mineralization at La Escondia. Geol. Soc. Am. Bull. 100, 1640–1656. http://dx.doi.org/10.1130/0016-7606(1988)1002.3.CO;2.

Baker, V.R., Partridge, J., 1986. Small martian valleys: Pristine and degraded morphology. J. Geophys. Res. 91 (B3), 3561–3572. http://dx.doi.org/10.1029/JB091iB03p03561.

Barnes, H.H. Jr., 1967. Roughness Characteristics of Natural Channels. U.S. Geol. Surv. Water-Supply Pap. 1849, U.S. Government Printing Office, Washington, DC.

Brakenridge, G.R., 1990. The origin of fluvial valleys and early geologic history, Aeolis quadrangle, Mars. J. Geophys. Res. 95, 17289–17308.

Carr, M.H., 2002. Elevations of water-worn features on Mars. J. Geophys. Res. 107 (E12), 5131. http://dx.doi.org/10.1029/2002JE001845.

Carr, M.H., Clow, G.D., 1981. Martian channels and valleys: Their characteristics, distribution, and age. Icarus 48, 91–117. http://dx.doi.org/10.1016/0019-1035(81)90156-1.

Chapman, M.G. (Ed.), 2007. The Geology of Mars: Evidence from Earth-based analogs. Cambridge University Press, p. 460.

Clarke, J.D.A., 2006. Antiquity of aridity in the Chilean Atacama Desert. Geomorphology 73, 101–114.

Craddock, R.A., Howard, A.D., 2002. The case for rainfall on a warm, wet early Mars. J. Geophys. Res. 107 (E11), 5111. http://dx.doi.org/10.1029/2001JE001505.

Craddock, R.A., Maxwell, T.A., Howard, A.D., 1997. Crater morphometry and modification in the Sinus Sabaeus and Margaritifer Sinus regions of Mars. J. Geophys. Res. 102, 13321–13340.

Craddock, R.A., Howard, A.D., Irwin III, R.P., Tooth, S., Williams, R.M., Chu, P.-S., 2012. Drainage network development in the Keanakāko'i Tephra, Kīlauea Volcano, Hawai'i: Implications for fluvial erosion and valley network formation on early Mars. J. Geophys. Res. 117, E08009. http://dx.doi.org/10.1029/2012JE004074.

Dingman, R.J., Galli, O.C., 1965. Geology and Ground-water Resources of the Pica Area, Tarapaca Province, Chile. U.S. Geol. Surv. Bull. 1189, U.S. Government Printing Office, Washington, DC.

Dunai, T.J., González-López, G.A., Juez-Larre, J., Carrizo, D., 2005. Oligocene–Miocene age of aridity in the Atacama Desert revealed by exposure dating of erosion-sensitive landforms. Geology 33, 321–324.

Dunne, T., 1980. Formation and controls of channel networks. Prog. Phys. Geogr. 4, 211–239.

Evenstar, L.A., Hartley, A.J., Stuart, F.M., Mather, A.E., Rice, C.M., Chong, G., 2009. Multiphase development of the Atacama Planation Surface recorded by cosmogenic ^{3}He exposure ages: Implications for uplift and Cenozoic climate change in western South America. Geology 37, 27–30. http://dx.doi.org/10.1130/G25437A.1.

Fassett, C.I., Head III, J.W., 2008. The timing of martian valley network activity: Constraints from buffered crater counting. Icarus 195, 61–89. http://dx.doi.org/10.1016/j.icarus.2007.12.009.

Gaidos, E., Marion, G., 2003. Geological and geochemical legacy of a cold early Mars. J. Geophys. Res. 108 (E6), 5055. http://dx.doi.org/10.1029/2002JE002000.

Galli, C., Dingman, R., 1962. Cuadrángulos Pica, Alca, Matilla y Chacarilla, con un estudio sobre los recursos de agua subterranean, Santiago, Chile, Instituto de Investigaciones Geológicas, 125p.

García, M., Gardeweg, M., Clavero, J., Hérail, G., 2004. Hoja Arica, Región de Tarapacá, Carta Geológica de Chile. Serie Geología Basica, No. 84, Escala 1:250,000, Servicio Nacional de Geología y Minería, Santiago, Chile.

García, M., Riquelme, R., Farías, M., Hérail, G., Charrier, R., 2011. Late Miocene–Holocene canyon incision in the western Altiplano, northern Chile: Tectonic or climatic forcing? J. Geol. Soc. (London, UK) 168, 1047–1060. http://dx.doi.org/10.1144/0016-76492010-134.

Gardner, T.W., 1983. Experimental study of knickpoint and longitudinal profile evolution in cohesive, homogeneous material. Geol. Soc. Am. Bull. 94, 664–672.

Gayo, E.M. et al., 2012. Late Quaternary hydrological and ecological changes in the hyperarid core of the northern Atacama Desert (~21°S). Earth-Sci. Rev. 113, 120–140. http://dx.doi.org/10.1016/j.earscirev.2012.04.003.

Goldspiel, J.M., Squyres, S.W., 1991. Ancient aqueous sedimentation on Mars. Icarus 89, 392–410. http://dx.doi.org/10.1016/0019-1035(91)90186-W.

Goldspiel, J.M., Squyres, S.W., Jankowski, D.G., 1993. Topography of small martian valleys. Icarus 105, 479–500. http://dx.doi.org/10.1006/icar.1993.1143.

Golombek, M.P. et al., 2006. Erosion rates at the Mars Exploration Rover landing sites and long-term climate change on Mars. J. Geophys. Res. 111, E12S10. http://dx.doi.org/10.1029/2006JE002754.

Grant, J.A., 2000. Valley formation in Margaritifer Sinus, Mars, by precipitation-recharged ground-water sapping. Geology 28, 223–226. http://dx.doi.org/10.1130/0091-7613(2000)28<223:VFIMSM>2.0.CO;2.

Grant, J.A., Wilson, S.A., 2011. Late alluvial fan formation in southern Margaritifer Terra, Mars. Geophys. Res. Lett. 38, L08201. http://dx.doi.org/10.1029/2011GL046844.

Gregory-Wodzicki, K.M., 2000. Uplift history of the central and northern Andes: A review. Geol. Soc. Am. Bull. 112, 1091–1105.

Gulick, V.C., 2001. Origin of the valley networks on Mars: A hydrological perspective. Geomorphology 37, 241–268. http://dx.doi.org/10.1016/S0169-555X(00)00086-6.

Gulick, V.C., Baker, V.R., 1990. Origin and evolution of valleys on martian volcanoes. J. Geophys. Res. 95, 14325–14344. http://dx.doi.org/10.1029/JB095iB09p14325.

Harrison, K.P., Grimm, R.E., 2005. Groundwater-controlled valley networks and the decline of surface runoff on early Mars. J. Geophys. Res. 110, E12S16. http://dx.doi.org/10.1029/2005JE002455.

Hartley, A.J., Chong, G., 2002. Late Pliocene age for the Atacama Desert: Implications for the desertification of western South America. Geology 30, 43–46. http://dx.doi.org/10.1130/0091-7613(2002) 0302.0.CO;2.

Hartley, A.J., Chong, G., Houston, J., Mather, A.E., 2005. 150 million years of climatic stability: Evidence from the Atacama Desert, northern Chile. J. Geol. Soc. (London, UK) 162, 421–424.
Haviv, I. et al., 2010. Evolution of vertical knickpoints (waterfalls) with resistant caprock: Insights from numerical modeling. J. Geophys. Res. 115, F03028. http://dx.doi.org/10.1029/2008JF001187.
Higgins, C.G., 1984. Piping and sapping; development of landforms by groundwater flow. In: LaFleur, R.G. (Ed.), Groundwater as a Geomorphic Agent. Allen and Unwin, Boston, pp. 18–58.
Hoke, G.D., Isacks, B.L., Jordan, T.E., Yu, J.S., 2004. Groundwater-sapping origin for the giant quebradas of northern Chile. Geology 32, 605–608.
Houston, J., 2001. La precipitación torrencial del año 2000 en Quebrada Chacarilla y el cálculo de recarga al acuífero Pampa Tamarugal, norte de Chile. Rev. Geol. Chile 28, 163–177.
Houston, J., 2002. Groundwater recharge through an alluvial fan in the Atacama Desert, northern Chile: Mechanisms, magnitudes and causes. Hydrol. Process. 16, 3019–3035.
Houston, J., 2006. Variability of precipitation in the Atacama Desert: Its causes and hydrological impact. Int. J. Climatol. 26, 2181–2198.
Houston, J., Hartley, A.J., 2003. The Central Andean west-slope rainshadow and its potential contribution to the origin of hyper-aridity in the Atacama Desert. Int. J. Climatol. 23, 1453–1464. http://dx.doi.org/10.1002/joc.938.
Howard, A.D., 1988. Introduction: Groundwater sapping on Mars and Earth. In: Howard, A.D., Kochel, R.C., Holt, H.E. (Eds.) Sapping Features of the Colorado Plateau: A Comparative Planetary Geology Field Guide. NASA [Spec. Publ.] SP 491, Washington, DC, pp. 1–5.
Howard, A.D., McLane, C.F., 1988. Erosion of cohesionless sediment by groundwater seepage. Water Resour. Res. 24, 1659–1674.
Howard, A.D., Kochel, R.C., Holt H.E. (Eds.), 1988. Sapping Features of the Colorado Plateau: A Comparative Planetary Geology Field Guide. NASA [Spec. Publ.] SP 491, Washington, DC, 108pp.
Howard, A.D., Moore, J.M., Irwin III, R.P., 2005. An intense terminal epoch of widespread fluvial activity on early Mars: 1. Valley network incision and associated deposits. J. Geophys. Res. 110, E12S14. http://dx.doi.org/10.1029/2005JE002459.
Hynek, B.M., Phillips, R.J., 2003. New data reveal mature, integrated drainage systems on Mars indicative of past precipitation. Geology 31, 757–760.
International Society for Rock Mechanics, 1978. Commission on standardization of laboratory and field tests, suggested methods for determining hardness and abrasiveness of rocks. Int. J. Rock Mech. Min. Geomech. Abstr. 15, 89–97.
Irwin III, R.P., Craddock, R.A., Howard, A.D., 2005. Interior channels in martian valley networks: Discharge and runoff production. Geology 336, 489–492.
Jakosky, B.M., Christensen, P.R., 1986. Global duricrust on Mars: Analysis of remote-sensing data. J. Geophys. Res. 91, 3547–3559.
Katz, O., Reches, Z., Roegiers, J.-C., 2000. Evaluation of mechanical rock properties using a Schmidt hammer. Int. J. Rock Mech. Min. 37, 723–728.
Komar, P.D., 1988. Sediment transport by floods. In: Baker, V.R., Kochel, R.C., Patton, P.C. (Eds.), Flood Geomorphology. Wiley-Interscience, New York, pp. 97–111.
Laity, J.E., 1983. Diagenetic controls on groundwater sapping and valley formation, Colorado Plateau, revealed by optical and electron microscopy. Phys. Geogr. 4, 103–125.
Laity, J.E., Malin, M.C., 1985. Sapping processes and the development of theater-headed valley networks on the Colorado Plateau. Geol. Soc. Am. Bull. 96, 203–217.
Lamb, M.P., Dietrich, W.E., 2009. The persistence of waterfalls in fractured rock. Geol. Soc. Am. Bull. 121, 1123–1134. http://dx.doi.org/10.1130/B26482.1.
Lamb, M.P., Howard, A.D., Johnson, J., Whipple, K.X., Dietrich, W.E., Perron, J.T., 2006. Can springs cut canyons into rock? J. Geophys. Res. 111, E07002. http://dx.doi.org/10.1029/2005JE002663.
Lamb, M.P., Howard, A.D., Dietrich, W.E., Perron, J.T., 2007. Formation of amphitheater-headed valleys by waterfall erosion after large-scale slumping on Hawai'i. Geol. Soc. Am. Bull. 119, 805–822. http://dx.doi.org/10.1130/B25986.1.
Lamb, M.P., Dietrich, W.E., Aciego, S.M., DePaolo, D.J., Manga, M., 2008a. Formation of Box Canyon, Idaho, by megaflood: Implications for seepage erosion on Earth and Mars. Science 320, 1067–1070.
Lamb, M.P., Dietrich, W.E., Venditti, J.G., 2008b. Is the critical Shields stress for incipient sediment motion dependent on channel-bed slope? J. Geophys. Res. 113, F02008. http://dx.doi.org/10.1029/2007JF000831.
Lamb, M.P., Mackey, B.H., Farley, K.A., 2014. Amphitheater-headed canyons formed by megaflooding at Malad Gorge, Idaho. Proc. Natl. Acad. Sci. USA 111, 57–62. http://dx.doi.org/10.1073/pnas.1312251111.
Lobkovsky, A.E., Smith, B.E., Kudrolli, A., Mohrig, D.C., Rothman, D.H., 2007. Erosive dynamics of channels incised by subsurface water flow. J. Geophys. Res. 112, F03S12. http://dx.doi.org/10.1029/2006JF000517.
Lumbroso, D., Gaume, E., 2012. Reducing the uncertainty in indirect estimates of extreme flash flood discharges. J. Hydrol. 414–415, 16–30. http://dx.doi.org/10.1016/j.jhydrol.2011.08.048.
Malin, M.C., 1976. Age of martian channels. J. Geophys. Res. 81, 4825–4845.
Malin, M.C., Carr, M.H., 1999. Groundwater formation of martian valleys. Nature 397, 589–591.
Mangold, N., Quantin, C., Ansan, V., Delacourt, C., Allemand, P., 2004. Evidence for precipitation on Mars from dendritic valleys in the Valles Marineris area. Science 305, 78–81. http://dx.doi.org/10.1126/science.1097549.
Marra, W.A., Braat, L., Baar, A.W., Kleinhans, M.G., 2014. Valley formation by groundwater seepage, pressurized groundwater outbursts and crater-lake overflow in flume experiments with implications for Mars. Icarus 232, 97–117.
Mars Channel Working Group, 1983. Channels and valleys on Mars. Geol. Soc. Am. Bull. 94, 1035–1054.
Masursky, H., Boyce, J.M., Dial, A.L., Schaber, G.G., Strobell, M.E., 1977. Classification and time of formation of martian channels based on Viking data. J. Geophys. Res. 82, 4016–4038. http://dx.doi.org/10.1029/JS082i028p04016.
Matthews, J.A., Shakesby, R.A., 1984. The status of the "Little Ice Age" in southern Norway: Relative-age dating of Neoglacial moraines with Schmidt Hammer and lichenometry. Boreas 15, 33–50.
Maxwell, T.A., Craddock, R.A., 1995. Age relations of martian highland drainage basins. J. Geophys. Res. 100, 11765–11780.
Mooney, H.A., Gulmon, S.L., Rundel, P.W., Ehleringer, J., 1980. Further observations on the water relations of *Prosopis tamarugo* of the northern Atacama Desert. Oecologia 44, 177–180.
Mortimer, C., 1980. Drainage evolution in the Atacama Desert of northern Chile. Rev. Geol. Chile 11, 3–28.
Parker, G., Wilcock, P.R., Paola, C., Dietrich, W.E., Pitlick, J., 2007. Physical basis for quasi-universal relations describing bankfull hydraulic geometry of single-thread gravel bed rivers. J. Geophys. Res. 112, F04005. http://dx.doi.org/10.1029/2006JF000549.
Pelletier, J.D., Baker, V.R., 2011. The role of weathering in the formation of bedrock valleys on Earth and Mars: A numerical modeling investigation. J. Geophys. Res. 116, E11007. http://dx.doi.org/10.1029/2011JE003821.
Perron, J.T., Hamon, J.L., 2012. Equilibrium form of horizontally retreating, soil-mantled hillslopes: Model development and application to a groundwater sapping landscape. J. Geophys. Res. 117, F01027. http://dx.doi.org/10.1029/2011JF002139.
Pieri, D.C., 1980. Geomorphology of martian valleys. In: Woronow, A. (Ed.), Advances in Planetary Geology, NASA/TM 81979, pp. 1–160.
Pinto, L., Hérail, G., Sepúlveda, S.A., Krop, P., 2008. A Neogene giant landslide in Tarapacá, northern Chile: A signal of instability of the westernmost Altiplano and palaeoseismicity effects. Geomorphology 102, 532–541.
Quade, J. et al., 2008. Paleowetlands and regional climate change in the central Atacama Desert, northern Chile. Quatern. Res. 69, 343–360. http://dx.doi.org/10.1016/j.yqres.2008.01.003.
Rech, J.A., Currie, B.S., Michalski, G., Cowan, A.M., 2006. Neogene climate change and uplift in the Atacama Desert, Chile. Geology 34, 761–764.
Schumm, S.A., Boyd, K.F., Wolff, C.G., Spitz, W.J., 1995. A groundwater sapping landscape in the Florida Panhandle. Geomorphology 12 (4), 281–297.
Selby, M.J., 1980. A rock-mass strength classification for geomorphic purposes: With tests from Antarctica and New Zealand. Z. Geomorphol. 24, 31–51.
Selby, M.J., 1993. Hillslope Materials and Processes, second ed. Oxford Univ. Press, Oxford, UK, 451pp.
Servicio Nacional de Geología y Minería, 2003. Mapa geologico de Chile: Version digital. Publication Geológica Digital, No. 4. versión 1.0, Base Geológica escala 1:1,000,000.
Strasser, M., Schlunegger, F., 2005. Erosional processes, topographic length-scales and geomorphic evolution in arid climatic environments: The 'Lluta collapse', northern Chile. Int. J. Earth Sci. (Geol. Rundsch.) 94, 433–446. http://dx.doi.org/10.1007/s00531-005-0491-2.
Strecker, M. et al., 2007. Tectonics and climate of the southern central Andes. Annu. Rev. Earth Planet. Sci. 35, 747–787.
Williams, R.M.E., Phillips, R.J., 2001. Morphometric measurements of martian valley networks from Mars Orbiter Laser Altimeter (MOLA) data. J. Geophys. Res. 106, 23737–23751.